

# Wearable Bioimpedance Sensor Characterization for Blood Flow Monitoring

Kaan Sel\*, Seyed Ali Ghazi Asgar\*, Deen Osman\*, Peiyun Wu\*, Roozbeh Jafari\*<sup>†</sup>

\*Department of Electrical and Computer Engineering, Texas A&M University, College Station, TX, USA

<sup>†</sup>School of Engineering Medicine, Texas A&M University, Houston, TX, USA

Email: ksel@tamu.edu, alighazi@tamu.edu, deenos25@tamu.edu, peiyun.wu@tamu.edu, rjafari@tamu.edu

**Abstract**—Bioimpedance is a powerful wearable sensing modality for continuous and non-invasive human deep tissue monitoring. When bioimpedance sensors are placed on the human body aligned with the underlying arteries – such as radial, ulnar, and digital – the impedance measurements show variations based on the changes in the artery dimensions due to the presence of blood pressure pulse waves. These variations can be leveraged to extract complex cardiovascular information, such as blood pressure. However, the level of impedance variations due to volumetric changes in the arteries is minimal (in the order of tens of mOhms) compared to the overall tissue impedances (in the order of hundreds of Ohms) requiring careful bioimpedance circuit and system design. In this paper, we provide comprehensive analyses of the bioimpedance sensor design requirements for arterial blood flow monitoring through numerical calculations, spice simulations, and experimental measurements. We provide analyses on signal-to-noise ratio (SNR) and effective number of bits (ENOB) requirements, indicating an 86dB SNR and 14-bit ENOB for high-resolution sensing. We believe this paper will further motivate the adoption of the promising wearable bioimpedance technology for applications of precision medicine.

**Keywords**—wearable bioimpedance sensing, biomedical system design, effective number of bits, blood flow, cuffless blood pressure monitoring

## I. INTRODUCTION

Emerging wearable technologies provide unprecedented opportunities for precision medicine, enabling continuous and non-invasive monitoring of specific health parameters ultimately advancing clinical decision-making. Among recent wearable technologies, bioimpedance sensors offer unique advantages due to their ability to perform deep tissue sensing, providing rich information on blood flow, respiration, hydration, muscle contraction, and other physiological activities [1]. A particular interest is their potential application in monitoring blood volumetric changes at peripheral arteries, where recent studies show that bioimpedance sensor measurements at wrists, chests, and fingers can be converted into complex cardiovascular biomarkers, such as blood pressure at clinical-level accuracies in lab-controlled experiments [2], [3]. However, the successful implementation and real-world deployment of bioimpedance sensors, particularly in clinical settings, still require a thorough understanding and characterization of the system-level requirements and limitations. This characterization includes understanding the analog and digital system design specifications necessary to obtain high-resolution blood flow measurements, investigating the impact of sensor dimensions and operating conditions, and electrode design considerations for reliable bioimpedance measurements. It also necessitates analyzing the requirements for translating bioimpedance measurements into complex cardiovascular parameters, such as blood pressure.

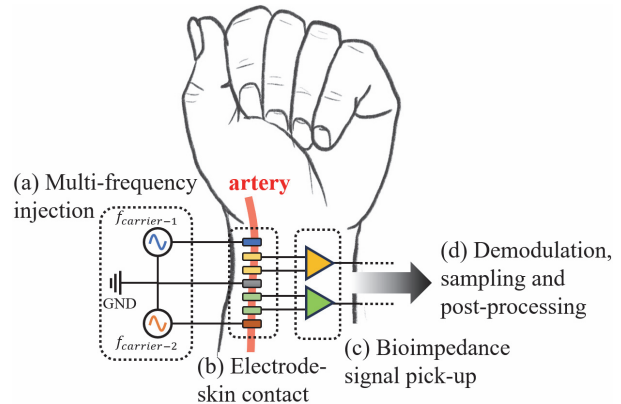


**Fig. 1** Overview of wearable bioimpedance sensing framework (a) Human tissue excitation with non-invasive electric current potentially at multiple frequencies (b) Electrode-skin contact aligned with an underlying artery for blood flow monitoring (c) Low-noise amplification of picked-up bioimpedance voltage signal. (d) Demodulation to obtain bioimpedance at baseband and sampling, followed by post-processing (e.g., feature engineering and machine learning for complex parameter estimation).

In the last decade or so, a body of work has been published on bioimpedance-based blood flow monitoring with sensors placed at various human body parts [4]–[6]. These existing studies primarily focus on the development of techniques and algorithms for complex parameter estimation from the pre-processed bioimpedance signal, rather than circuits and system considerations used for successful signal acquisition. We believe that the community will greatly benefit from a thorough characterization of the requirements involved in bioimpedance sensor design and utilization for the proper adoption of the technology.

In this paper, we present a comprehensive analysis of the requirements for wearable bioimpedance sensors, in particular for measuring arterial blood flow and volumetric changes (Fig. 1). This paper aims to fill the gaps in the knowledge and provide a roadmap to the community pertaining to the high-fidelity utilization of bioimpedance sensors through a detailed analysis of the electrode interface, circuit design, and signal processing considerations. We present numerical calculations and experimental measurements of noise figures and resolutions of sensor components to assess the requirements and limitations posed by each component involved in bioimpedance sensing. In addition, we provide analyses on the impact of effective number of bits of digital conversion on the captured signal morphology, which directly impacts feature engineering for complex parameter estimation.

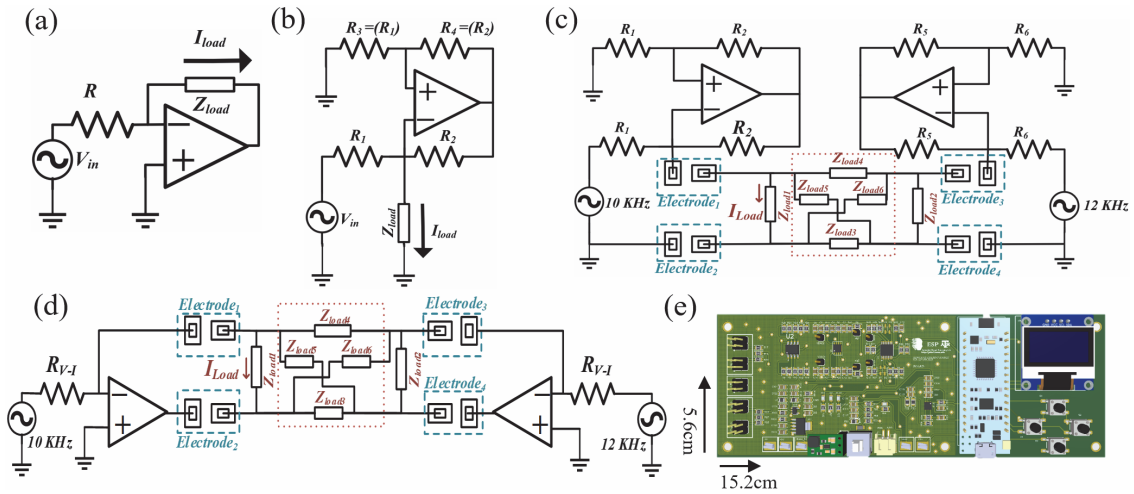


**Fig. 2** (a) Floating load voltage-to-current converter schematic. (b) Howland current source schematic. (c) Howland current source for multi-frequency current injection equivalent schematic. (d) Floating load voltage-to-current converter circuit for multi-frequency injection. (e) PCB for testing Howland Current source with display and buttons to control the frequency and amplitude of the signals.

The rest of the paper is organized as follows. In Section II, we provide bioimpedance electrode placement and size considerations specifically for blood flow monitoring, and hardware considerations for tissue excitation required for bioimpedance sensing. Then, in Section III, we provide simulation and experimental results for different circuit paradigms along with analyses on system signal-to-noise ratio (SNR) and effective number of bits (ENOB) for analog front-end (AFE) and digital signal processing (DSP) blocks. Our conclusion is provided in Section IV.

## II. METHODS

### A. Bioimpedance Electrode Considerations

Bioimpedance sensing requires a minimum of four electrical contacts established with the human skin through skin electrodes. The first pair of electrodes is used for injecting a high-frequency electrical signal – often in the form of an alternating current (AC) – and the second pair is used for sensing the modulated voltage based on the tissue composition and electrical characteristics. To capture a traveling blood pressure pulse wave, the optimal signal quality is obtained when the voltage-sensing electrodes are placed directly on top of the targeted artery [7]. On the other hand, signal injection electrodes can be placed parallel to the voltage sensing electrodes, or can be placed in a single axis with the voltage sensing pair along the artery, based on the feasibility constraints set by the wearable form factor [2], [7]. It has been shown that higher separation between sensing electrodes yields a higher bioimpedance signal amplitude, whereas a lower separation between current injection electrodes will improve the localization of the arterial pulse wave. For wrist-worn applications, a 5-10mm separation between the sensing electrode pair and a 1-3mm separation between the injection electrodes and the adjacent sensing electrodes is typical.

The type of electrode material used for skin contact plays a crucial role in terms of electrical contact quality. Wet Ag/AgCl electrodes offer low contact impedance allowing for tissue excitation with higher current amplitude, however, they show poor integrability to wearable devices. Silver (Ag) dry-contact electrodes, on the other hand, are suitable for wearable

device integration, yet they suffer from high electrode-skin impedances, which will affect the measurement system design and operation conditions. For example, utilizing dry electrode sizes of 9mm<sup>2</sup> would yield over 15k $\Omega$  impedance at 10kHz [8]. For 1mA current injected at the tissue – corresponding to the maximum allowed current amplitude at this frequency – this would mean a 30V peak-to-peak voltage swing at the power supply, much higher than the typical wearable system supply ranges. The electrode-skin impedance is inversely proportional to the electrode-skin contact area as well as the injection frequency, hence depending on the system requirements different operating conditions and electrode sizes should be selected.

### B. Tissue Excitation for Bioimpedance Sensing

Bioimpedance sensing depends on four-point sensing, *a.k.a.* Kelvin sensing. Kelvin sensing technique separates the injection and sensing contact points from each other to isolate the load impedance from the lead and contact impedances. Hence, the picked-up voltage ( $V_{sense}$ ), in this case, can be expressed as;

$$V_{sense} = I_{inject} \times Z_{tissue} \quad (1)$$

Here,  $I_{inject}$  and  $Z_{tissue}$  refer to the injected AC signal and the tissue impedance, respectively. To effectively capture  $Z_{tissue}$  and therefore its variations due to blood volumetric changes in the arteries from  $V_{sense}$ ,  $I_{inject}$  should either have a constant peak amplitude or be fully measured through a current sensing circuit. Constant amplitude current injection with programmable amplitude and frequency is recommended to avoid the circuitry required for current monitoring.

#### 1) Single-Frequency Operation

A digital-to-analog converter (DAC) generates the programmability of the shape, amplitude, and frequency of the injected signal. Once generated, this signal needs to be converted into a current signal with constant amplitude. For single-frequency operations, the “floating load voltage-to-current converter” circuit provides effective conversion (Fig. 2a) [9]. This circuit is simple and only requires one resistor and one OpAmp, where the injected current is equal to

$V_{DAC}/R_{V-I}$  due to the negligible current inflow to OpAmp input leads. Although this circuit only requires two electrodes to inject the current, adding a GND electrode can further increase the SNR by over 7 dB [10].

## 2) Multi-Frequency Operation

The floating load voltage to the current converter circuit works well for single-frequency injection, however, it cannot be used for multi-frequency injection. As shown in Fig. 2d, when two of these injection circuits are placed on the body, due to the finite tissue impedances between two sites ( $Z_{load,3}$ ,  $Z_{load,4}$ ,  $Z_{load,5}$ , and  $Z_{load,6}$ ), there would be current leakage through the output of one of the OpAmps to the feedback loop of the second OpAmp distorting the injected current. To overcome this issue, we recommend using the Howland current source [11], [12], as shown in Fig. 2b-c,e. Here, when  $R_1 = R_3$  and  $R_2 = R_4$ ,  $I_{load}$  can be determined as follows:

$$I_{load} = \frac{V_{in}}{R_1} \quad (2)$$

## C. Signal-to-Noise Requirements for Bioimpedance Sensing

The voltage difference occurs due to the injected current passing through the tissue is a superposition of different tissue layers, including muscle, fat, tendon, bone, and blood vessels. For a wrist-worn bioimpedance sensor, this impedance reaches around  $100\Omega$  magnitude (at 10kHz injection). When the sensors are aligned with the underlying arteries (e.g., radial), the impedance shows quasiperiodic variations due to the changes in blood volume. These changes are very small, at around  $50m\Omega$ . To effectively capture morphological features from this small signal, we recommend the system to have at least a  $3-5m\Omega$  resolution. Therefore, the measurement system has to be carefully designed with SNR and ENOB considerations. The specific recommendations are shared in this section.

### 1) Input Signal Power

From the sensing voltage equation (1), the output voltage  $V_{sense}$  is directly proportional to the injected current  $I_{inject}$ . Hence, a higher current amplitude will result in a stronger signal, which will inherently improve system SNR. However, there are practical limits to allowable injection current amplitude.

#### a) Safety considerations

There are safety standards by ANSI/AAMI for the amplitude and frequency of signals that can be injected into the human body [13]. According to these standards, at 10kHz the maximum allowable current injection is 1mA rms. Increasing the frequency to 100kHz will allow for a 1-fold increase in the maximum allowable amplitude of the current.

#### b) Power supply considerations

The skin impedance for dry electrodes with  $25mm^2$  contact area ranges between  $5k\Omega$  and  $10k\Omega$  at 10kHz. For full range (i.e., class A) operation,  $I_{inject} \times Z_{tissue}$  should be less than  $V_{supply}$ . Otherwise, the injection signal will experience clipping.

### 2) Analog Front-End Considerations

To measure a  $5m\Omega$  change in bioimpedance, the required resolution is a maximum  $5\mu V$  noise floor at the maximum allowable 1mA injection.

The bioimpedance AFE for the current injection consists of a DAC, followed by a bandpass filter and a voltage-to-current (V-to-I) converter. We use a low-noise 16-bit DAC (DAC8811, Texas Instruments) in our system to generate a programmable voltage signal. This DAC has a low noise profile of  $12nV/\sqrt{Hz}$ . A high-precision OpAmp (OPA2277, Texas Instrument) with a low input voltage noise density of  $8nV/\sqrt{Hz}$  (at 10kHz) is used for the filter. The voltage-to-current converter uses a precision OpAmp (OPA211, Texas Instruments) with a low  $1.1nV/\sqrt{Hz}$  noise density. Assuming a 20Hz bandwidth around the baseband of blood volumetric changes, the combination of both integrated circuits (IC) introduces a  $\sim 95nV$  noise combined. This noise becomes negligible (compared with  $5\mu V$ ).

The voltage sensing AFE consists of an instrumentational amplifier (IA) for signal amplification over the full dynamic range. We use a low-noise IA (AD8421, Analog Devices), with a  $3.2nV/\sqrt{Hz}$  maximum input voltage noise at 1 kHz, resulting in a  $\sim 14nV$  noise floor at 20Hz bandwidth. In addition, this IC is low power with a 2.3 mA maximum supply current and has excellent AC specifications of over 100 dB common-mode rejection ratio (CMRR) at 10 kHz with a gain over 10.

The amplified voltage signal is modulated at the injection frequency (typically at 1-100kHz). The blood volumetric changes in the bioimpedance signal should be brought to the baseband for post-processing based on analog or digital demodulation techniques. To achieve high-configurability, our system uses digital demodulation, where the signal is passed through an anti-aliasing filter and sampled with an analog-to-digital converter (ADC) at 93,750Hz which is  $\sim 9$  times higher than the carrier frequency,  $f_c$ , of 10kHz. However, for the final bioimpedance system with fixed design specifications, we recommend analog demodulation prior to the sampling to bring the bioimpedance signal to the baseband, as this will decrease the sampling constraint on Nyquist frequency from  $2 \times f_c$  to the bandwidth of interest ( $< 1kHz$ ). Once the signal representing tissue impedance and its changes is brought to the baseband, the selection of ADC resolution becomes crucial to decide the system SNR performance. However, the ADC resolution reduces due to the noise and distortion in the physical circuit. The effective resolution of the system in bits (ENOB) is used to determine SNR as,

$$SNR = 6.02 ENOB + 1.76dB \quad (3)$$

For the target resolution of 86dB (corresponding to a  $5\mu V$  noise floor for  $\sim 100mV$  signal at 1mA injection), a 14-bit ENOB is needed. Hence, at least 16-bit or higher resolution ADC is required. ENOB can further be improved by using oversampling and averaging technology if ADC noise can be approximated as white noise. Based on the theory of noise and oversampling [14], [15], the relationship between the oversampling frequency and the ADC resolution is,

$$f_{os} = 4^w f_s \quad (4)$$

where  $w$  is the number of additional bits of resolution desired,  $f_s$  is the original sampling frequency, and  $f_{os}$  is the oversampling frequency. It shows that each additional required bit of resolution can be achieved via oversampling by

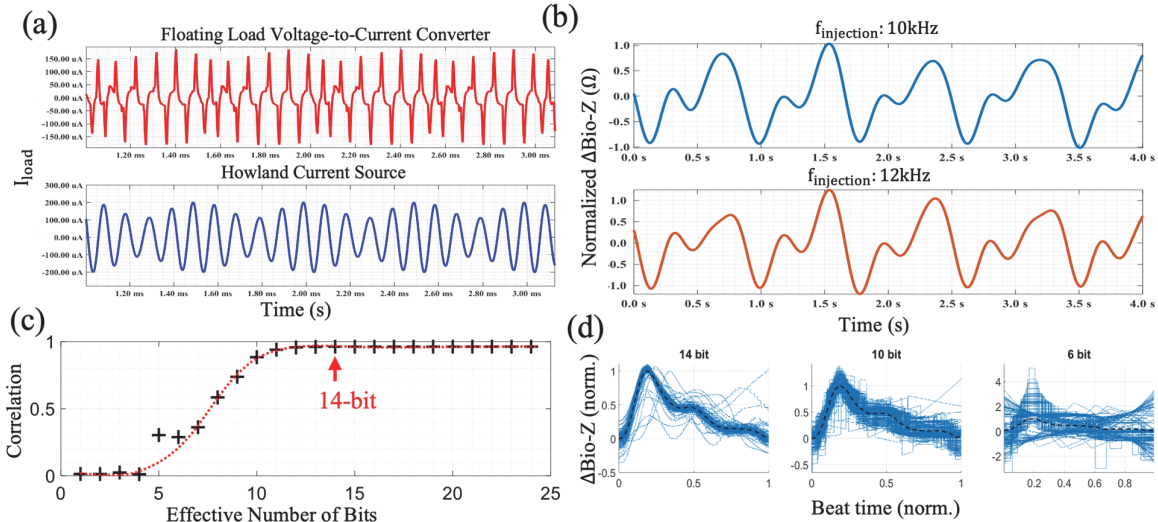


**Fig. 3** Experimental and simulation results (a) LTspice simulations for multi-frequency current injection techniques. (b) Bioimpedance signal collected at 10kHz (top) and 12kHz (bottom) current injection using Howland Current source. (c) Beat-to-beat waveform correlation with the group mean w.r.t. the change in effective number of bits (ENOB) used for sampling. (d) Overlapping normalized bioimpedance waveforms based on 14, 10, and 6 ENOB, from left to right, respectively. A decrease in ENOB causes loss of resolution in beat-to-beat waveform.

a factor of four, and each additional bit will add approximately 6dB of resolution.

### III. RESULTS & DISCUSSION

#### A. Multi-Frequency Injection Analysis

We run LTspice simulations (transient analysis) of the two approaches: Howland current source and floating load voltage-to-current converter circuits presented in Fig. 2c and d, respectively, to assess the injection current stability during multi-frequency operation. Here, the resistor values for the Howland circuit and floating load V-I circuit are selected as  $R_1 = R_4 = 5k\Omega$ ,  $R_2 = R_3 = 1k\Omega$ , and  $R_{V-I} = 5k\Omega$ , whereas the electrode-skin impedances are selected based on previous studies [10], [16] and all load-impedances are picked as  $50\Omega || (50\Omega + 50nF)$ . Fig. 3a shows the simulation results, where with Howland current circuit (bottom plot) the injected current is not distorted, and both harmonics are well-preserved, whereas the floating load V-I circuit (top plot) results in a distorted signal.

In addition to LTspice simulations, we performed experimental validation of the multi-frequency operation using Howland current board (Fig. 2e) with one-minute-long experiments performed on a healthy participant, who provided their consent under the IRB approval IRB2017-0086D by Texas A&M University. The Howland current board is used to simultaneously inject current at 10kHz and 12kHz frequencies, while a previously developed benchtop bioimpedance board [2] is used to obtain the bioimpedance signal at two channels. The electrode skin contact is established through seven wet Ag/AgCl electrodes placed at the participant's wrist with 5mm separation aligned with their radial artery. The outer electrodes and the middle electrode are used for current injection, while the remaining electrodes are used to capture bioimpedance signal at two channels (Fig. 1). Fig. 3b shows the bioimpedance waveforms simultaneously captured at two carrier frequencies using this circuit configuration, providing a consistent quasi-periodic (at heart rate) bio-impedance morphology.

#### B. ENOB vs. Signal Morphology Analysis

To demonstrate the importance of ENOB selection, we performed an analysis on a 3-minute snippet of a bioimpedance signal collected at the participant's wrist, with the bioimpedance sensor aligned with the underlying radial artery. For this analysis, we demodulated the bioimpedance signal that is sampled with a 24-bit ADC (ADS1278, Texas Instruments) and performed bit-shifting to simulate the decrease in the ENOB used in signal sampling for a case of analog demodulation. Fig. 3c shows the decrease in signal consistency after 14 bits, calculated using the average Pearson's correlation coefficient obtained from the beat-by-beat segmented bioimpedance signals and the mean waveform morphology. In addition, Fig. 3d shows segmented waveforms normalized, inverted, and overlapped when sampled with 14, 10, and 6 bits indicating the impact of decreasing ENOB in signal resolution, leading to a loss of morphological characteristics past 14 bits.

### IV. CONCLUSION

This work provides a characterization of important modules involved in designing high-fidelity bioimpedance sensing systems. Although certain calculations provided here can show variations based on the sensing location, electrode selection, and operating conditions, the presented recommendations should be carefully considered in designing wearable bioimpedance sensors and systems for blood flow and volume monitoring.

#### ACKNOWLEDGMENT

This work was supported in part by the U.S. National Institute of Health Grant 1R01EB028106. Any opinions, findings, conclusions, or recommendations expressed in this material are those of the authors and do not necessarily reflect the views of the funding organizations.

## REFERENCES

- [1] S. Grimnes and O. G. Martinsen, *Bioimpedance and bioelectricity basics*. Academic press, 2011.
- [2] K. Sel, D. Osman, N. Huerta, A. Edgar, R. I. Pettigrew, and R. Jafari, "Continuous cuffless blood pressure monitoring with a wearable ring bioimpedance device," *npj Digit. Med.*, vol. 6, no. 1, p. 59, Mar. 2023.
- [3] B. Ibrahim and R. Jafari, "Cuffless blood pressure monitoring from a wristband with calibration-free algorithms for sensing location based on bio-impedance sensor array and autoencoder," *Sci. Rep.*, vol. 12, no. 1, pp. 1–14, 2022.
- [4] K. Sel, D. Osman, and R. Jafari, "Non-invasive cardiac and respiratory activity assessment from various human body locations using bioimpedance," *IEEE open J. Eng. Med. Biol.*, vol. 2, pp. 210–217, Jun. 2021.
- [5] H. C. Lukaski, "Evolution of bioimpedance: a circuitous journey from estimation of physiological function to assessment of body composition and a return to clinical research," *Eur. J. Clin. Nutr.*, vol. 67, no. 1, pp. S2–S9, 2013.
- [6] D. G. Jakovljevic, M. I. Trenell, and G. A. MacGowan, "Bioimpedance and bioreactance methods for monitoring cardiac output," *Best Pract. Res. Clin. Anaesthesiol.*, vol. 28, no. 4, pp. 381–394, 2014.
- [7] K. Sel, N. Huerta, M. S. Sacks, and R. Jafari, "Parametric Modeling of Human Wrist for Bioimpedance-Based Physiological Sensing," in *ICASSP 2022 - 2022 IEEE International Conference on Acoustics, Speech and Signal Processing (ICASSP)*, 2022, pp. 1161–1165.
- [8] D. Kireev *et al.*, "Fabrication, characterization and applications of graphene electronic tattoos," *Nat. Protoc.* 2021 165, vol. 16, no. 5, pp. 2395–2417, Apr. 2021.
- [9] A. H. Ar-Rawi, M. Moghavvemi, and W. M. A. Wan-Ibrahim, "Comparing between three current source circuits for using in bio electrical impedance design," in *2009 International Conference for Technical Postgraduates (TECHPOS)*, 2009, pp. 1–4.
- [10] K. Sel, B. Ibrahim, and R. Jafari, "ImpediBands: Body Coupled Bio-Impedance Patches for Physiological Sensing Proof of Concept," *IEEE Trans. Biomed. Circuits Syst.*, vol. 14, no. 4, pp. 757–774, Aug. 2020.
- [11] H. Yazdani, M. Mosayebi Samani, and A. Mahanm, "Characteristics of the Howland current source for bioelectric impedance measurements systems," in *2013 20th Iranian Conference on Biomedical Engineering (ICBME)*, 2013, pp. 189–193.
- [12] B. Ibrahim, A. Talukder, and R. Jafari, "Multi-source Multi-frequency Bio-impedance Measurement Method for Localized Pulse Wave Monitoring," in *2020 42nd Annual International Conference of the IEEE Engineering in Medicine & Biology Society (EMBC)*, 2020, pp. 3945–3948.
- [13] T. Master and T. Mark, *Medical electrical equipment Part 1: General requirements for basic safety and essential performance ANSI/AAMI ES60601-1:2005/A1:2012*. ANSI/AAMI ES60601-1:2005/A1:2012: ANSI/AAMI ES60601-1:2005/A1:2012, 2012.
- [14] A. V Oppenheim, *Discrete-time signal processing*. Pearson Education India, 1999.
- [15] J. C. Candy and G. C. Temes, "Oversampling methods for A/D and D/A conversion," *Oversampling delta-sigma data Convert.*, pp. 1–25, 1992.
- [16] J. Xu, S. Mitra, C. Van Hoof, R. F. Yazicioglu, and K. A. A. Makinwa, "Active Electrodes for Wearable EEG Acquisition: Review and Electronics Design Methodology," *IEEE Rev. Biomed. Eng.*, vol. 10, pp. 187–198, 2017.